

Subspace-Based Identification of Linear Time-Varying System

Z. Y. Shi*

*Nanjing University of Aeronautics and Astronautics,
Nanjing, People's Republic of China*

S. S. Law†

*Hong Kong Polytechnic University,
Hong Kong, People's Republic of China*

and

H. N. Li‡

*Nanjing University of Aeronautics and Astronautics,
Nanjing, People's Republic of China*

DOI: 10.2514/1.28555

A physical parameter identification method for the linear time-varying system is presented in this paper. For an arbitrarily time-varying system, a series of Hankel matrices are established directly from the combined measurements of displacement, velocity, and acceleration together with the input excitations from a single experiment with the system. The time-varying equivalent state-space system matrices of the structure at each time instance are then identified by singular value decomposition using the free or random responses. A time-varying transformation matrix for transforming the identified equivalent system matrices into the physical system matrices is developed to determine the mass, stiffness, and damping matrices. Details of the proposed approach are investigated with a two degrees-of-freedom spring-mass-damper system with three kinds of time-varying parameters. Numerical results show that the proposed method is accurate and effective in identifying time-varying physical parameters.

Nomenclature

b	=	input shape matrix
C_a, C_v, C_d	=	output index matrices for the measurement of acceleration, velocity, and displacement, respectively
$E(t)$	=	time-dependant damping matrix of the system
$G(k+1, k)$	=	discrete-time state transition matrix
$H(k)$	=	discrete-time input influence matrix
I	=	unit matrix
$K(t)$	=	time-dependant stiffness matrix of the system
$M(t)$	=	time-dependant mass matrix of the system
n_i	=	the number of input force signals
n_o	=	the number of output signals
$T(t)$	=	transformation matrix
$U(k)$	=	input influence matrix
$u(t)$	=	input force vector
$x(t)$	=	displacement response vector
$\dot{x}(t)$	=	velocity response vector
$\ddot{x}(t)$	=	acceleration response vector
$Y(k)$	=	Hankel matrix
$y(k)$	=	output vector at discrete-time step k
$y(t)$	=	output vector
$z(k)$	=	state vector at discrete-time step k
$z(t)$	=	state vector
$\Gamma(k)$	=	observability matrix of the system at discrete-time step k

Superscripts

H	=	Hermitian transpose of a matrix
T	=	transpose of a matrix
$+$	=	Moore–Penrose inverse of a matrix

I. Introduction

LINEAR time-invariant (LTI) models are usually appropriate and commonly used to describe the dynamic behavior of most structural systems. Many damage detection methods have been developed based on the LTI model by confirming changes in the modal parameters of structures between predamage and postdamage vibration tests [1–5]. However, a structural system always accumulates damage due to service loading or environmental excitations. Some mechanical parameters of the systems are time dependent, such as stiffness, damping, and so on, and the dynamic characteristics of structural systems are time varying. Under such circumstances, a linear time-varying (LTV) model would better capture the instantaneous dynamic behaviors and track the time-varying parameters of structural systems for assessing the conditions of the system or to diagnose for any potential failure. The identification of linear time-varying systems has received increasing attention recently due to its important application in electrical, communication, control, mechanic, and civil engineering.

Existing methods for identifying modal parameters can be categorized as time-domain methods and frequency-domain methods. Frequency-domain methods are popular and predominant in engineering practice. Time-domain methods are usually useful and necessary in the analysis of complex structures with many close modes and multichannel measurement. These methods included the Ibrahim time-domain method [6,7] and the polyreference method [8]. State-space system identification methods offer reliable models for complex multivariable dynamic systems directly from measured data. The Eigensystem realization algorithm (ERA) [9,10] was developed to identify modal parameters using noisy measurement data from the Markov parameters. The singular value decomposition (SVD) of the Hankel matrix was used to extract the system matrices. A recursive algorithm of the ERA was later proposed in [11]. Liu and

Received 26 October 2006; revision received 26 March 2007; accepted for publication 26 March 2007. Copyright © 2007 by the American Institute of Aeronautics and Astronautics, Inc. All rights reserved. Copies of this paper may be made for personal or internal use, on condition that the copier pay the \$10.00 per-copy fee to the Copyright Clearance Center, Inc., 222 Rosewood Drive, Danvers, MA 01923; include the code 0001-1452/07 \$10.00 in correspondence with the CCC.

*Professor, College of Aerospace Engineering; zyshi@nuaa.edu.cn.

†Associate Professor, Department of Civil and Structural Engineering; cecslaw@polyu.edu.hk.

‡Research Student, College of Aerospace Engineering.

Miller [12] proposed the observability range space extraction identification algorithm based on the Q -Markov covariance equivalent realization [13] and the ERA identification algorithms. A SVD-based identification method with several important applications was discussed in [14]. Overschee and Moore [15] proposed the numerical algorithm for subspace state-space system identification. Different types of subspace-based methods could be found in [16–18]. Chui and Maciejowski [19] provided an algorithm to find stable approximation to a least-squares problem to ensure the stability of the subspace methods. Huang et al. [20,21] developed the identification algorithm to extract the equivalent state system matrices based on the ERA and the autoregressive with an exogenous model using the combined measurements of displacement, velocity, and acceleration data. Also a modal identification system based on the vector backward autoregression with an exogenous model was proposed in [22].

However, all the aforementioned studies have been limited to the identification of LTI systems. Some efforts have been made to develop identification algorithms for time-varying linear or nonlinear systems based on different approaches, such as the Hilbert–Huang transform method [23–25], the adaptive tracking method [26–29], the wavelet-based method [30,31], and the state-space method [32–34]. Compared with the identification algorithm for the LVI system, existing identification methods for the LTV system still exhibit many weaknesses and are not ready for real application. Further investigation and development of a robust and practical identification algorithm for the LTV system is necessary and desirable.

For using the state-space method, some authors have extended identification algorithms from LTI systems to LTV systems. Shokoohi and Silverman [35] developed a solution at consecutive time instances to identify the state-space model formed using impulse response data. Verhaegen and Yu [36] extended this solution to the identification of the state-space model to extract successive discrete transition matrices of a LTV system based on a subspace-based algorithm from an ensemble of input and output data. A typical subspace-based discrete-time state-space technique was proposed to identify linear time-varying systems [32]. The algorithm focuses on the time-varying transition matrix that shares the same eigenvalues as the original transition matrix. A series of Hankel matrices is formed from an ensemble set of responses obtained through multiple experiments on the system with the same time-varying behavior. Singular value decomposition is used to extract observability range spaces. The shift invariance structure preserved in two successive extracted subspaces is used to estimate the time-varying transition matrix at a time instance. Liu [33] further introduced the concept of pseudomodal parameters to characterize the dynamics of LTV systems, and extended his previously proposed algorithm to include the forced responses in the identification of the pseudomodal parameters. Experimental verification studies on an axially moving cantilever beam were subsequently addressed in [34].

Existing identification algorithms for the LTV system based on the state-space method have the assumption that multiple experiments are conducted on the system with parameters undergoing the same variation. This assumption is not feasible with some LTV systems, especially for the mechanical system or civil structural system. To overcome this limitation, a subspace-based identification algorithm for the linear time-varying system is developed by using a set of free response data or random excitation response data. A nonsingular transformation matrix is proposed to extract real system matrices from equivalent system matrices estimated by the proposed subspace-based identification algorithm. The paper is organized as follows. Section II introduces the state-space model of the LTV system. Section III develops a subspace-based identification algorithm to identify discrete transition matrices and system matrices using only a set of free response sequences or random excitation response sequences. A transformation matrix is developed to extract the equivalent system matrices in Sec. IV. Section V presents several numerical examples to illustrate the proposed method. Section VI gives a brief conclusion.

II. State-Space Model of the LTV System

The equation of motion of a p -degrees-of-freedom (DOF) LTV system can be expressed as

$$M(t)\ddot{x}(t) + E(t)\dot{x}(t) + K(t)x(t) = bu(t) \quad (1)$$

The output equation for the same p -DOF LTV system can be represented as

$$y(t) = C_a\ddot{x}(t) + C_v\dot{x}(t) + C_d x(t) \quad (2)$$

where $y(t)$ can be a combination of different types of responses such as $\ddot{x}(t)$, $\dot{x}(t)$, and $x(t)$.

A state vector consisting of displacement and velocity vectors is defined as

$$z(t) = \{x(t) \quad \dot{x}(t)\}^T \quad (3)$$

Equations (1) and (2) can be transformed into the state-space equation of motion and output as follows:

$$\dot{z}(t) = A(t)z(t) + B(t)u(t) \quad (4)$$

$$y(t) = C(t)z(t) + D(t)u(t) \quad (5)$$

In the above equations, $A(t)$ is the $2p \times 2p$ system matrix, $B(t)$ is the $2p \times n_i$ input matrix, $C(t)$ is the $n_o \times 2p$ output influence matrix, and $D(t)$ is the $n_o \times n_i$ direct transmission matrix, respectively. The matrices $A(t)$, $B(t)$, $C(t)$, and $D(t)$ are expressed as

$$A(t) = \begin{bmatrix} 0 & I \\ -M^{-1}(t)K(t) & -M^{-1}(t)E(t) \end{bmatrix} \quad (6a)$$

$$B(t) = [0 \quad M^{-1}(t)b]^T \quad (6b)$$

$$C(t) = \begin{bmatrix} C_d - C_a M^{-1}(t)K(t) \\ C_v - C_a M^{-1}(t)E(t) \end{bmatrix}^T \quad (6c)$$

$$D(t) = C_a M^{-1}(t)b \quad (6d)$$

If the excitation and response signals are measured at discrete-time instances with a sampling interval Δt , the continuous time domain can be discretized into a finite number of time steps. Let $t_k = k\Delta t$ ($k = 1$ to N). The response $z(t_k)$ at step k is simply described as $z(k)$. The corresponding discrete-time state-space representation can be transformed from Eqs. (4) and (5) as follows:

$$z(k+1) = G(k+1, k)z(k) + H(k)u(k) \quad (7)$$

$$y(k) = C(k)z(k) + D(k)u(k) \quad (8)$$

in which $G(k+1, k)$ is the $2p \times 2p$ discrete-time state transition matrix from step k to step $(k+1)$, and $H(k)$ is the $2p \times n_i$ input influence matrix at step k .

It is noted that matrices $G(k+1, k)$ and $H(k)$ are time varying, and they can be obtained as [37]

$$G(k+1, k) \approx \exp[A(k)\Delta t] \quad (9)$$

$$H(k) \approx [G(k+1, k) - I]A^{-1}(k)B(k) \quad (10)$$

III. Subspace-Based Identification Algorithm for the LTV System

This section is concerned with the identification algorithm for the LTV system. A subspace-based identification is proposed based on the discrete-time state-space model using one set of free vibration response data or random excitation response data.

It is assumed that only one set of experimental data has been obtained from the LTV system. The excitation and response signals are described by $u(k)$ and $y(k)$, ($k = 1, 2, \dots, N$), respectively. A general block Hankel matrix $Y(k)$ and input influence matrix $U(k)$ are formed using the output response vectors and input force vectors as

$$Y(k) = \begin{bmatrix} y(k) & y(k+1) & \cdots & y(k+n-1) \\ y(k+1) & y(k+2) & \cdots & y(k+n) \\ \vdots & \vdots & \ddots & \vdots \\ y(k+m-1) & y(k+m) & \cdots & y(k+m+n-2) \end{bmatrix}_{mn_0 \times n} \quad (11)$$

$$U(k) = \begin{bmatrix} u(k) & u(k+1) & \cdots & u(k+n-1) \\ u(k+1) & u(k+2) & \cdots & u(k+n) \\ \vdots & \vdots & \ddots & \vdots \\ u(k+m-1) & u(k+m) & \cdots & u(k+m+n-2) \end{bmatrix}_{mn_i \times n} \quad (12)$$

where m and n are two selected coefficients that guarantee the observability and controllability of the system. Subscripts mn_0 and mn_i denote the products of m and n_0 , and m and n_i , respectively.

A. Identification Algorithm Based on Free Vibration Response Data

For the free vibration system, the discrete-time state-space equations can be simplified from Eqs. (7) and (8) as

$$z(k+1) = G(k+1, k)z(k) \quad (13)$$

$$y(k) = C(k)z(k) \quad (14)$$

Using Eqs. (13) and (14), the Hankel matrix in Eq. (11) can be written as

$$Y(k) = \Gamma(k)Z(k) \quad (15)$$

where $Z(k) = [z(k) \ z(k+1) \ z(k+2) \ \cdots \ z(k+n-1)]_{2p \times n}$, and the observability matrix $\Gamma(k)$ of the system is

$$\Gamma(k) = \begin{bmatrix} C(k) & C(k+1) & \cdots \\ C(k+1)G(k+1, k) & C(k+2)G(k+2, k+1) & \cdots \\ C(k+2)G(k+2, k) & C(k+3)G(k+3, k+1) & \cdots \\ \vdots & \vdots & \vdots \\ C(k+m-1)G(k+m-1, k) & C(k+m)G(k+m, k+1) & \cdots \end{bmatrix}_{mn_0 \times 2np} \quad (16)$$

An assumption is made that the system undergoes the same time-varying properties during the time intervals; that is, $[k \ k+m-1]$, $[k+1 \ k+m]$, \dots , $[k+n-1 \ k+n+m-2]$. The observability matrix of the system can then be simplified as

$$\Gamma(k) = \begin{bmatrix} C(k) \\ C(k+1)G(k+1, k) \\ C(k+2)G(k+2, k) \\ \vdots \\ C(k+m-1)G(k+m-1, k) \end{bmatrix}_{mn_0 \times 2p} \quad (17)$$

The Hankel matrix $Y(k+1)$ can be formed using response sequences from $k+1$ to $k+m+n+1$, and a similar observability matrix $\Gamma(k+1)$ is obtained as

$$\Gamma(k+1) = \begin{bmatrix} C(k+1) \\ C(k+2)G(k+2, k+1) \\ C(k+3)G(k+3, k+1) \\ \vdots \\ C(k+m)G(k+m, k+1) \end{bmatrix}_{mn_0 \times 2p} \quad (18)$$

If $\Gamma_2(k+1)$ is taken to be the first $m-1$ block rows of $\Gamma(k+1)$ and $\Gamma_1(k)$ to be the last $m-1$ block rows of $\Gamma(k)$, it is easily found that

$$\Gamma_2(k+1)G(k+1, k) = \Gamma_1(k) \quad (19)$$

and

$$G(k+1, k) = [\Gamma_2(k+1)]^+ [\Gamma_1(k)] \quad (20)$$

In practical implementation, the SVD method is used to decompose the two Hankel matrices $Y(k)$ and $Y(k+1)$ as

$$Y(k) = R(k) \sum(k) V^T(k), \quad (21)$$

$$Y(k+1) = R(k+1) \sum(k+1) V^T(k+1)$$

in which $R(k)$ and $V(k)$ are the orthogonal matrices with $mn_0 \times mn_0$ dimension and $n \times n$ dimension, respectively, $\sum(k) = \text{diag}[\sigma(k)_1, \sigma(k)_2, \dots, \sigma(k)_s, 0 \cdots 0]$ is the $mn_0 \times n$ diagonal singular value matrix. When the free vibration signals are free of noise, the number of the nonzero singular values s is equal to $2p$. When the response signals are contaminated by noise, the number of the nonzero singular values will be equal to $\min(mn_0, n)$. It is known that the diagonal matrix $\sum(k)$ contains the first $2p$ significantly large singular values and the rest are small when the signal-to-noise ratio is high or moderate. It can also be proved [32] that

$$R_s(k) \sum_s^2(k) R_s^H(k) \approx \Gamma(k) [Z(k) Z^H(k)] \Gamma(k) \quad (22)$$

in which $R_s(k)$ is formed using the first s columns of $R(k)$, $\sum_s(k)$ is formed from the first s singular values of matrix $\sum(k)$, and s is equal to $2p$. Equation (22) shows that $R_s(k)$ forms an orthogonal basis for the observability range space.

$$R_s(k) = \bar{\Gamma}(k) \quad (23)$$

in which matrix $\bar{\Gamma}(k)$ has the same range space as that of matrix $\Gamma(k)$. The corresponding discrete-time state transition matrix $\bar{G}(k+1, k)$ can be obtained as

$$\bar{G}(k+1, k) = [R_{s2}(k+1)]^+ [R_{s1}(k)] \quad (24)$$

where $R_{s2}(k)$ and $R_{s1}(k)$ are formed using the first $(m-1)n_0$ block rows of $R_s(k+1)$ and the last $(m-1)n_0$ block rows of $R_s(k)$, respectively. $\bar{G}(k+1, k)$ is similarly equivalent to the state transition matrix $G(k+1, k)$ through a transformation matrix, which

will be introduced in the next section. Also, the equivalent system matrix $\bar{A}(k)$ can be solved using Eq. (9) at the discrete-time instant k .

B. Identification Algorithm Based on Random Excitation Response Data

The assumption that the system exhibits the same time-varying properties during different time intervals remains valid in the following derivation. When random excitation response signals are used, the Hankel matrix in Eq. (11) and the input influence matrix in Eq. (12) can be rewritten based on Eqs. (7) and (8) as

$$Y(k) = \Gamma(k)Z(k) + \Theta(k)U(k) \quad (25)$$

in which the observability matrix of the system is the same as that in Eq. (17), and $\Theta(k)$ is a $mn_0 \times mn_i$ matrix with the i th block matrix in the j th column of the matrix given by

$$\Theta_{ij}(k) = \begin{cases} 0, & i < j \\ D(k+i-1) & i = j \\ C(k+i-1)H(k+j-1) & i = j+1 \\ C(k+i-1)G(k+i-1, k+j)H(k+j-1) & i > j+1 \end{cases} \quad (26)$$

An important step of the algorithm is to extract the range space of the observability matrix. To extract the observability range space, the part of output $Z(k)$ that does not originate from the state $Y(k)$ needs to be eliminated. In other words, the second term on the right-hand side of Eq. (25) has to be removed. Thus, a full row rank matrix $U^\perp(k)$ is defined such that $U^\perp(k)$ is normal to $U(k)$ or $U(k)U^\perp(k) = 0$ [33], with

$$U^\perp(k) = I - U^T(k)[U(k)U^T(k)]^{-1}U(k) \quad (27)$$

Postmultiply Eq. (25) with $U^\perp(k)$, we have

$$Y(k)U^\perp(k) = [\Gamma(k)Z(k) + \Theta(k)U(k)]U^\perp(k) = \Gamma(k)Z(k)U^\perp(k) \quad (28)$$

The range space of the observability matrix is then obtained from $Y(k)U^\perp(k)$ as

$$\bar{\Gamma}(k) = \text{range}[Y(k)U^\perp(k)] = \begin{bmatrix} \bar{C}(k) \\ \bar{C}(k+1)\bar{G}(k+1, k) \\ \bar{C}(k+2)\bar{G}(k+2, k) \\ \vdots \\ \bar{C}(k+m-1)\bar{G}(k+m-1, k) \end{bmatrix} \quad (29)$$

If the response data from the time instances $(k+1)$ to $(k+m)$ are used, matrices $Y(k+1)$, $\Gamma(k+1)$, $\Theta(k+1)$, and $U(k+1)$ are related as

$$Y(k+1) = \Gamma(k+1)Z(k+1) + \Theta(k+1)U(k+1) \quad (30)$$

The observability matrix $\bar{\Gamma}(k+1)$ can also be obtained in a similar way as

$$\bar{\Gamma}(k+1) = \begin{bmatrix} \bar{C}(k+1) \\ \bar{C}(k+2)\bar{G}(k+2, k+1) \\ \bar{C}(k+3)\bar{G}(k+3, k+1) \\ \vdots \\ \bar{C}(k+m)\bar{G}(k+m, k+1) \end{bmatrix} \quad (31)$$

Also if matrix $\bar{\Gamma}_2(k+1)$ is taken to be the first $m-1$ block rows of $\bar{\Gamma}(k+1)$ and $\bar{\Gamma}_1(k)$ to be the last $m-1$ block rows of $\bar{\Gamma}(k)$, respectively, it is easily found that

$$\begin{aligned} \bar{\Gamma}_2(k+1)\bar{G}(k+1) &= \bar{\Gamma}_1(k) \quad \text{and} \\ \bar{G}(k+1, k) &= [\bar{\Gamma}_2(k+1)]^+[\bar{\Gamma}_1(k)] \end{aligned} \quad (32)$$

where $[\cdot]^+$ denotes the Moore–Penrose inverse of $[\cdot]$.

In practical implementation, the SVD method is used to extract the range space of $\bar{\Gamma}(k)$ or $\bar{\Gamma}(k+1)$.

$$Y(k)U^\perp(k) = R(k)\Sigma(k)V^T(k) \quad (33)$$

$$Y(k+1)U^\perp(k+1) = R(k+1)\Sigma(k+1)V^T(k+1) \quad (34)$$

According to the properties of the SVD, the first $s = 2p$ column of $R(k)$ and $R(k+1)$ give a set of the base vectors for the range space of $\bar{\Gamma}(k)$ and $\bar{\Gamma}(k+1)$, respectively.

$$R_s(k) = \bar{\Gamma}(k) \quad (35)$$

$$R_s(k+1) = \bar{\Gamma}(k+1) \quad (36)$$

The discrete-time state transition matrix $\bar{G}(k+1, k)$ can then be obtained as

$$\bar{G}(k+1, k) = [R_{s2}(k+1)]^+[R_{s1}(k)] \quad (37)$$

where $R_{s2}(k)$ and $R_{s1}(k)$ are formed using the first $(m-1)n_0$ block rows of $R_s(k+1)$ and the last $(m-1)n_0$ block rows of $R_s(k)$, respectively. $\bar{G}(k+1, k)$ is similarly equivalent to the state transition matrix $G(k+1, k)$ through a transformation matrix, which will be introduced in the next section.

To extract the range space of matrix $\Theta(k)$, another simple formulation of $\Gamma^\perp(k)$ is given similar to matrix $U^\perp(k)$ as

$$\Gamma^\perp(k) = I - \Gamma(k)[\Gamma^T(k)\Gamma(k)]^{-1}\Gamma^T(k) \quad (38)$$

Premultiplying Eq. (25) by $\Gamma^\perp(k)$ results in

$$\Gamma^\perp(k)Y(k) = \Gamma^\perp(k)[\Gamma(k)Z(k) + \Theta(k)U(k)] = \Gamma^\perp(k)\Theta(k)U(k) \quad (39)$$

Thus

$$\Theta(k) = [\Gamma^\perp(k)]^+ \Gamma^\perp(k)Y(k)[U(k)]^+ \quad (40)$$

Because matrix $\bar{\Gamma}(k)$ has the same range space as matrix $\Gamma(k)$, a similar equation can be written as

$$\bar{\Theta}(k) = [\bar{\Gamma}^\perp(k)]^+ \bar{\Gamma}^\perp(k)Y(k)[U(k)]^+ \quad (41)$$

where $\bar{\Theta}(k)$ gives the same base vectors for the range space of $\Theta(k)$. When matrix $\bar{\Gamma}(k)$ is calculated using Eq. (35), matrix $\bar{\Theta}(k)$ can be obtained from Eq. (41).

Let $\bar{\Theta}_1(k)$ be formed using the first n_i column of matrix $\bar{\Theta}(k)$, and $\bar{\Theta}_2(k)$ be formed using the last $(m-1)n_0$ rows of matrix $\bar{\Theta}_1(k)$. Matrix $\bar{\Theta}_2(k)$ can be expressed as

$$\begin{aligned} \bar{\Theta}_2(k) &= \begin{bmatrix} \bar{C}(k+1)\bar{H}(k) \\ \bar{C}(k+2)\bar{G}(k+2, k+1)\bar{H}(k) \\ \bar{C}(k+3)\bar{G}(k+3, k+1)\bar{H}(k) \\ \vdots \\ \bar{C}(k+m-1)\bar{G}(k+m-1, k+1)\bar{H}(k) \end{bmatrix} \\ &= \bar{\Gamma}_2(k)\bar{H}(k) \end{aligned} \quad (42)$$

Thus

$$\bar{H}(k) = [\bar{\Gamma}_2(k)]^+ \bar{\Theta}_2(k) \quad (43)$$

$\bar{H}(k)$ is similarly equivalent to the input influence matrix $H(k)$ through a transformation matrix, which will be introduced in the next

section. Furthermore, the system matrix $\tilde{A}(k)$ and the input matrix $\tilde{B}(k)$ can be solved using Eqs. (9) and (10) at the discrete-time instance k when the matrices $\tilde{G}(k+1, k)$ and $\tilde{H}(k)$ are calculated from Eqs. (37) and (43), respectively.

IV. Extraction of Equivalent System Matrix

As mentioned in the above section, matrix pair $\tilde{A}(k)$ and $\tilde{B}(k)$ estimated using the proposed identification algorithm is equivalent to the matrix pair $A(k)$ and $B(k)$ of the system. The equivalent matrix pair $\tilde{A}(k)$ and $\tilde{B}(k)$ has the same dynamic characteristics as $A(k)$ and $B(k)$. To obtain the system matrix $A(k)$ and the input matrix $B(k)$, a nonsingular transformation matrix is introduced [33].

$$z(t) = T(t)z_m(t) = \begin{bmatrix} T_1(t) \\ T_2(t) \end{bmatrix} z_m(t) \quad (44)$$

in which $z_m(t)$ is a new state vector describing the state-space of the estimated model and $T(t)$ is the transformation matrix. Hence, the following relationships can be obtained:

$$A(t) = T(t)\tilde{A}(t)T^{-1}(t) \quad (45a)$$

$$B(t) = T(t)\tilde{B}(t) \quad (45b)$$

$$C(t) = \tilde{C}(t)T^{-1}(t) \quad (45c)$$

$$D(t) = \tilde{D}(t) \quad (45d)$$

Substituting Eqs. (6a) and (44) into Eq. (45a), we get

$$T_2(t) = T_1(t)\tilde{A}(t) \quad (46)$$

$$M^{-1}(t)K(t)T_1(t) + M^{-1}(t)E(t)T_2(t) = -T_2(t)\tilde{A}(t) \quad (47)$$

Substituting Eqs. (6b) and (44) into Eq. (45b), we get

$$-C_a M^{-1}(t)[K(t)T_1(t) + E(t)T_2(t)] + C_d T_1(t) + C_v T_2(t) = \tilde{C}(t) \quad (48)$$

Substituting Eqs. (46) and (47) into Eq. (48), we get

$$C_d T_1(t) + C_v T_1(t)\tilde{A}(t) + C_a T_1(t)\tilde{A}^2(t) = \tilde{C}(t) \quad (49)$$

Matrix $T_1(t)$ can then be obtained as

$$T_1(t) = C_d^+ \tilde{C}(t) + C_v^+ \tilde{C}(t)\tilde{A}^{-1}(t) + C_a^+ \tilde{C}(t)[\tilde{A}^{-1}(t)]^2 \quad (50)$$

Based on Eqs. (46) and (50), the transformation matrix $T(t)$ in Eq. (44) can be rewritten as

$$T(t) = \begin{bmatrix} C_d^+ \tilde{C}(t) + C_v^+ \tilde{C}(t)\tilde{A}^{-1}(t) + C_a^+ \tilde{C}(t)[\tilde{A}^{-1}(t)]^2 \\ C_d^+ \tilde{C}(t)\tilde{A}(t) + C_v^+ \tilde{C}(t) + C_a^+ \tilde{C}(t)\tilde{A}^{-1}(t) \end{bmatrix} \quad (51)$$

The system matrix and the input matrix can then be easily calculated using Eqs. (45a) and (45b). Defining matrices $\tilde{A}(k)$ and $\tilde{B}(k)$ as the estimated system and input matrices, respectively, they can be obtained as

$$\tilde{A}(k) = \begin{bmatrix} \tilde{A}_{11}(k) & \tilde{A}_{12}(k) \\ \tilde{A}_{21}(k) & \tilde{A}_{22}(k) \end{bmatrix} = \begin{bmatrix} 0 & I \\ -\tilde{M}^{-1}(k)\tilde{K}(k) & -\tilde{M}^{-1}(k)\tilde{E}(k) \end{bmatrix} \quad (52)$$

$$\tilde{B}(k) = \begin{bmatrix} \tilde{B}_1(k) \\ \tilde{B}_2(k) \end{bmatrix} = \begin{bmatrix} 0 \\ \tilde{M}^{-1}(k)b \end{bmatrix} \quad (53)$$

in which $\tilde{M}(k)$, $\tilde{K}(k)$, $\tilde{E}(k)$ are the estimated mass, stiffness, and damping matrices at the discrete-time instant k , respectively, and they can be obtained from Eqs. (52) and (53) as

$$\tilde{M}(k) = b[\tilde{B}_2(k)]^+ \quad (54)$$

$$\tilde{K}(k) = -b[\tilde{B}_2(k)]^+ \tilde{A}_{21}(k) \quad (55)$$

$$\tilde{E}(k) = -b[\tilde{B}_2(k)]^+ \tilde{A}_{22}(k) \quad (56)$$

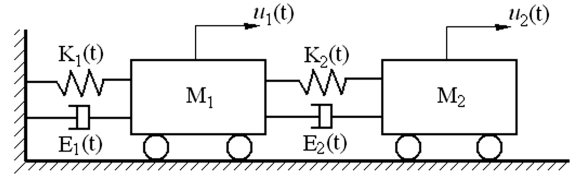
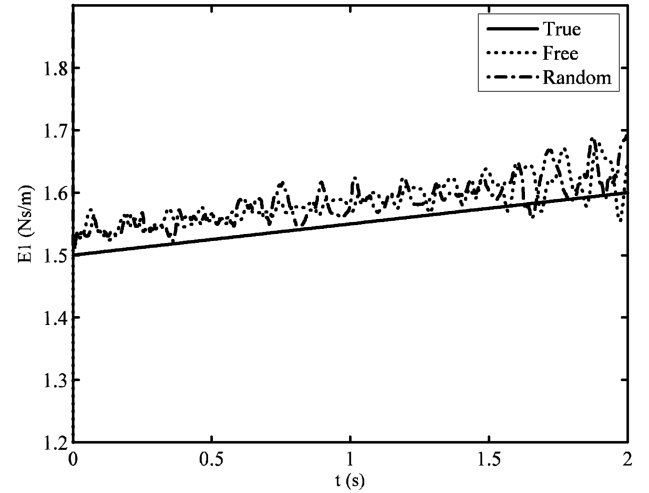
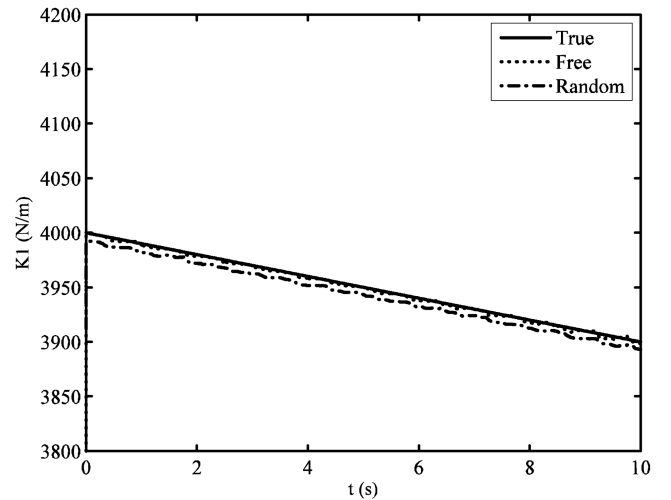


Fig. 1 Two degrees of freedom lumped mass model.



a)



b)

Fig. 2 Comparison of true values and the identified results estimated for the smoothly time-varying system.

V. Simulation Results

To illustrate the effectiveness and accuracy of the proposed identification algorithm, a lumped mass model with the two degrees-of-freedom system shown in Fig. 1 is selected for the case study. The lumped mass coefficients of the model are assumed constant, which are $m_1 = m_2 = 1$ kg. The damping and stiffness coefficients of the model are assumed as time varying. Two kinds of response sequences are calculated from the numerical solution of the equation of motion using the Newmark method. One is the free vibration response which is simulated with an initial velocity and acceleration at the two lumped masses as $\dot{x}_0 = 1.0$ m/s and $\ddot{x}_0 = 1.0$ m/s². Another is the random response from the two lumped masses under normally distributed random excitation. The sampling rate of time series data is 1000 Hz. Acceleration responses are used to estimate time-varying parameters with the proposed identification algorithm.

The numerical examples cover three different types of time-varying systems. They are 1) smoothly varying system: the damping and stiffness variations are $E_1(t) = 1.5 + 0.05t$ Ns/m, $E_2(t) = 1.2$ Ns/m, $K_1(t) = 4000 - 50t$ N, $K_2(t) = 1600$ N; 2) abruptly varying system: the variations are $E_1(t) = 1.5$ Ns/m, $E_2(t) = 1.2$ Ns/m, $K_1(t)$ changes abruptly at $t = 1.0$ s from the original value of 3000 N to the new value of 2600 N, $K_2(t) = 1600$ N; and 3) periodically varying system: the damping and stiffness variations are $E_1(t) = 1.0$ Ns/m, $E_2(t) = 0.8$ Ns/m, $K_1(t) = 4000 + 50 \sin(3t)$ N, $K_2(t) = 3000 + 50 \sin(3t)$ N.

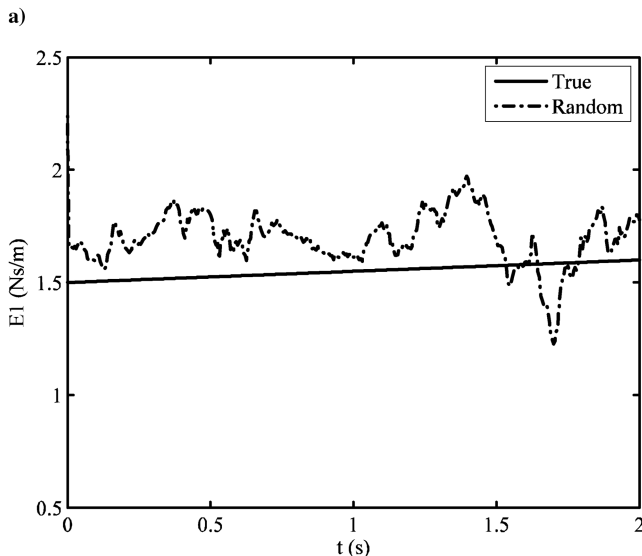
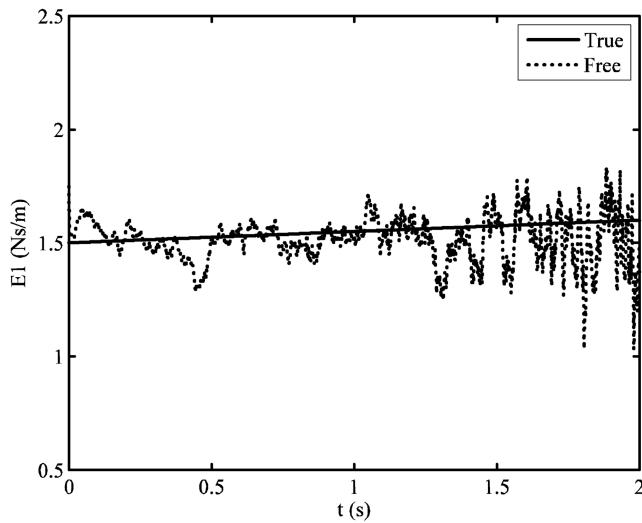


Fig. 3 Comparison of true value and the identified damping coefficient $E_1(t)$ estimated for the smoothly time-varying system (SNR = 50).

For the smoothly time-varying system, damping and stiffness coefficients are estimated with the proposed identification algorithm using free vibration response signals and random response signals. The response data are not corrupted with noise. Figure 2 shows a comparison between the true value (solid line) and the identified results from free response data (dotted line) and random response data (dash-dotted line). The estimated damping and stiffness coefficients are shown in Figs. 2a and 2b, respectively. Results show that the proposed identification algorithm has a good capability of tracking the parametric changes of the system. The estimated results from using the free vibration responses are more accurate than those estimated by using the random responses during the whole identification time period.

For demonstrating the ability of the proposed method with noisy data, the response signals are assumed to be contaminated with zero mean Gaussian noise. The signal-to-noise ratio (SNR) is defined as

$$\text{SNR} = srs/sn$$

where srs denotes the standard deviation of the response signal and sn is the standard deviation of the added noise. In the actual implementation, the numerical response is calculated and its srs is found. sn is determined from a given SNR. A standard Gaussian white noise with a unit standard deviation is then generated and multiplied with the value sn . It is then added to the response to produce the “measured” response.

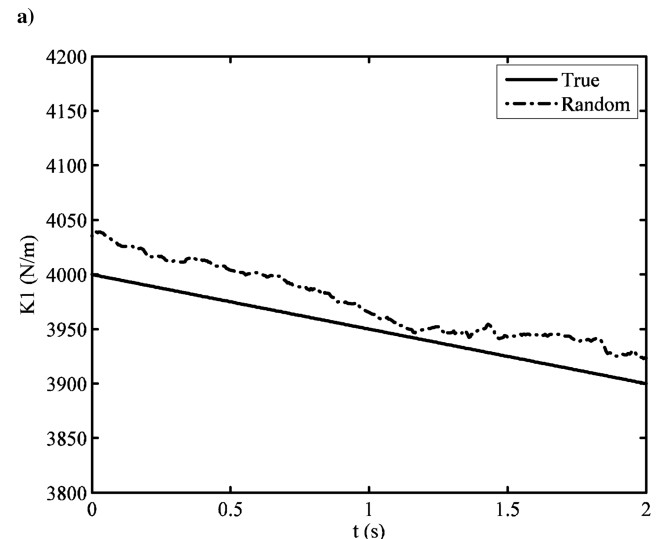
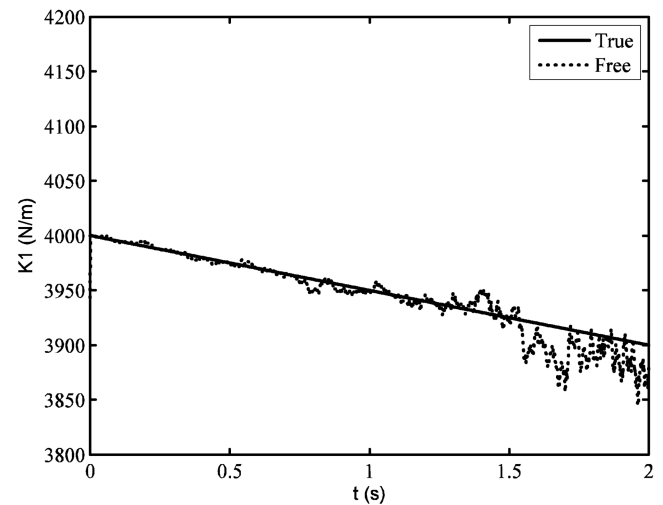


Fig. 4 Comparison of true value and the identified stiffness coefficient $K_1(t)$ estimated for the smoothly time-varying system (SNR = 50).

We assume all response data are corrupted by noise with a SNR equal to 50. The above three different types of time-varying systems are studied and the identified results are shown in Figs. 3–7. The identified result using free vibration response is denoted with a dotted line, the result identified using random vibration response is denoted with a dash-dotted line, and the corresponding true value is denoted with a solid line in each figure.

Figures 3 and 4 show the estimated damping coefficients and stiffness coefficients of the smoothly time-varying system, respectively. It can be observed that the identified damping and stiffness coefficients are close to the corresponding true values when using free vibration response data or random response data. The present identification algorithm has a good tracking behavior on the smooth change of the damping and stiffness of the system when the response data are corrupted with noise. It is also observed that the estimated results from free vibration response in Figs. 3a and 4a are closer to the true values than those estimated from random response in Figs. 3b and 4b. The identified results in Figs. 3a and 4a turn out to have larger fluctuations at the end of the time duration. It is due to the fact that the free vibration response suffers attenuation under the action of the system damping.

Figure 5 shows the identified results for the abruptly time-varying system. The abrupt jump in the stiffness coefficient of the system can be tracked using the proposed identification algorithm using either free vibration response data or using random response data. The estimated results with the dotted line shown in Fig. 5a or estimated results with the dash-dotted line shown in Fig. 5b show an abrupt

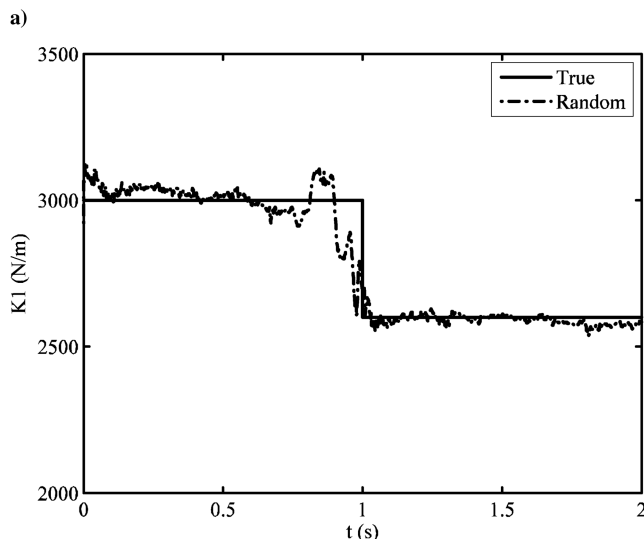
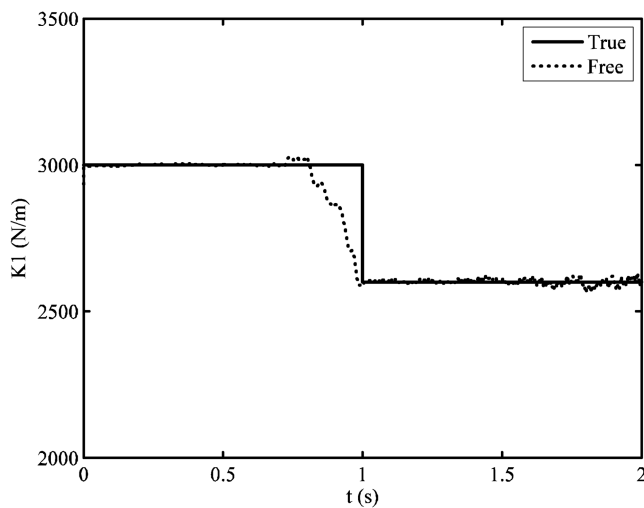


Fig. 5 Comparison of true value and the identified stiffness coefficient $K_1(t)$ estimated for the abruptly time-varying system (SNR = 50).

change in the stiffness from 3000 to 2600 N, which matches with the corresponding true changes denoted with the solid line at $t = 1.0$ s. However, it is noted that there exists a larger identification error at the time instance when the system stiffness has an abrupt change. This indicates that the proposed algorithm has poor capability in tracking abrupt variations due to the assumption that the system exhibits the same time-varying properties during the time intervals in the development of the parameter identification equation in Secs. III.A and III.B.

The identified results for the periodically time-varying stiffness coefficients $K_1(t)$ and $K_2(t)$ are shown in Figs. 6 and 7, respectively. It can be seen that the dotted lines (estimated by using free response data) in Figs. 6a and 7a or the dash-dotted lines (estimated by using random response data) in Figs. 6b and 7b are found varying around the solid lines (the true values). The proposed method is shown to be capable of tracking the periodical change of stiffness during the whole time duration. It is noted that there is a phase shift between the estimated result and the corresponding true value in Figs. 6 and 7. This phase shift is due to the identification being conducted using the range of data in the time intervals, that is $[k \ k + m - 1]$, $[k + 1 \ k + m]$, \dots , $[k + n - 1 \ k + n + m - 2]$, and so on, and the results are plotted at the k , $k + 1$, \dots , and so on, time instances.

For further demonstration of the effect of noise on the identified results, Figs. 8a and 8b compare the corresponding true values with the identified damping and stiffness terms for the smoothly time-varying system. They are estimated using random response data corrupted with noise with different SNR values of 100, 50, 30, and

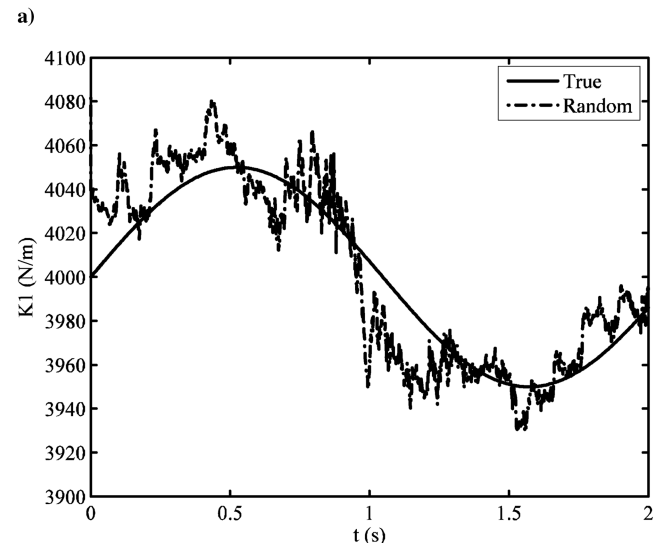
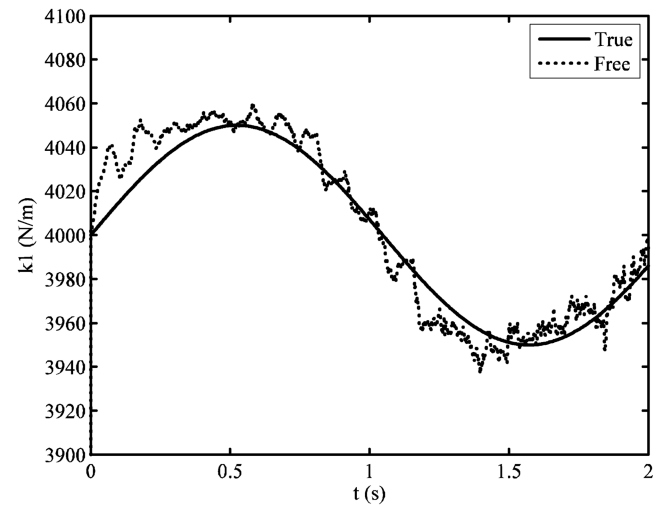
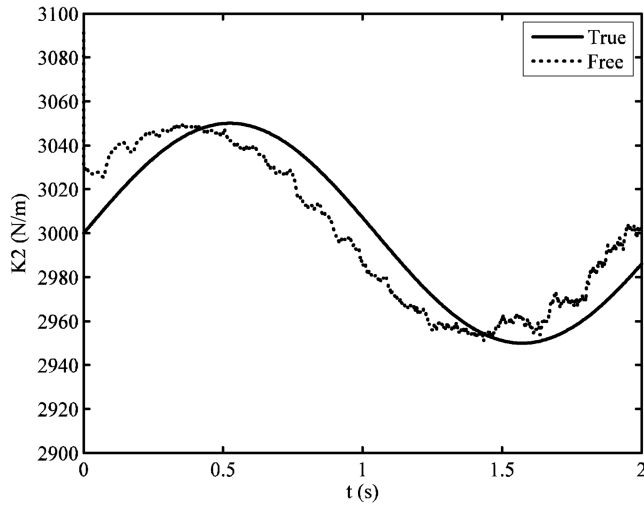
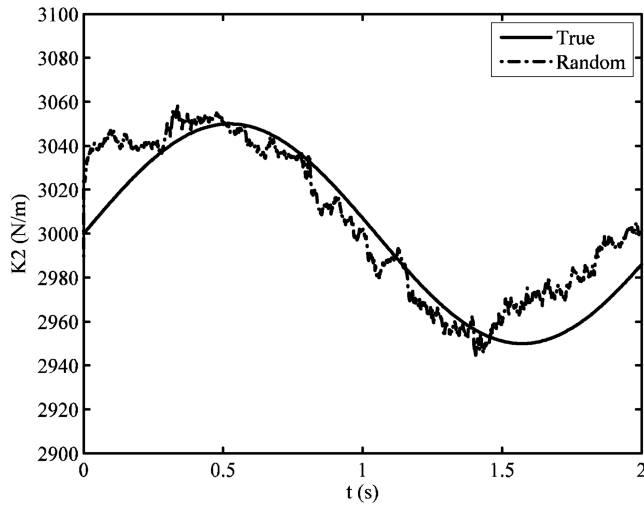


Fig. 6 Comparison of true value and the identified stiffness coefficient $K_1(t)$ estimated for the periodically time-varying system (SNR = 50).



a)



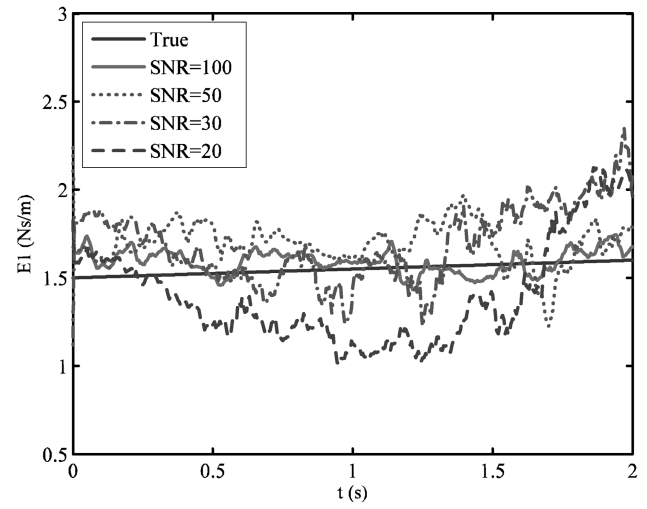
b)

Fig. 7 Comparison of true value and the identified stiffness coefficient $K_2(t)$ Estimated for the periodically time-varying system (SNR = 50).

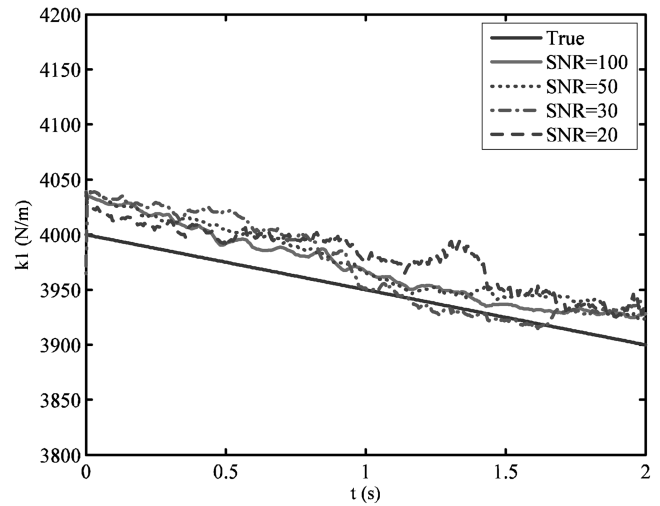
20. Results show that higher SNR response gives higher identification accuracy. To have a quantitative discussion, the mean absolute percentage error (MAPE) is defined as

$$\text{MAPE} = \frac{1}{N} \sum_{i=1}^N \frac{|P_i - \tilde{P}_i|}{P_i} \times 100\%$$

in which P_i, \tilde{P}_i denote the true value and the identified value at the i th time instance, N is the total sample number. The MAPE of the time-varying parameters of the above mentioned time-varying systems is calculated using free response or random response and listed in Table 1. It is noted that the errors (MAPE) increase with a decrease in SNR for all three types of time-varying systems by using the free responses or the random responses. The errors of identification of the stiffness coefficients have good accuracy with all the MAPE values



a)



b)

Fig. 8 Comparison of true value and the identified results estimated using corrupted random response with difficult SNR for the smoothly time-varying system.

smaller than 2%. However, the errors of identification for the damping coefficients are larger with some of them larger than 15%.

VI. Conclusions

This paper addresses the identification of time-varying system based on the state-space formulation. Existing methods based on multiple experiments are improved to one that is based on only a single experiment. A subspace-based physical parameter identification algorithm is developed via free or random responses in this paper. A series of Hankel matrices is established from only a set of combined measurements of displacement, velocity, and acceleration response signals. The time-varying equivalent state-space system matrices at each time instance are then estimated using singular value decomposition technique. A new time-varying transformation

Table 1 Error of identification (MAPE) with noisy data

SNR	From free response					From random response				
	Smooth		Abrupt		Periodical	Smooth		Abrupt		Periodical
	$E_1, \%$	$K_1, \%$	$K_1, \%$	$K_1, \%$	$K_2, \%$	$E_1, \%$	$K_1, \%$	$K_1, \%$	$K_1, \%$	$K_2, \%$
100	9.051	0.334	0.843	0.205	0.374	6.493	0.375	0.708	0.297	0.401
50	17.621	0.325	0.944	0.204	0.409	9.562	0.401	1.109	0.339	0.406
30	27.361	0.288	1.046	0.397	0.374	15.691	0.512	0.861	0.639	0.585
20	31.073	0.522	1.173	0.380	0.434	18.255	0.612	1.106	0.689	0.624

matrix is proposed to transform the identified equivalent system matrices into the physical system matrices to determine the mass, stiffness and damping matrices. This proposed identification approach is the restriction to linear time-varying systems different from the cited nonparametric approaches [27,28] that can deal with time-varying linear or nonlinear systems.

A two-degrees-of-freedom lumped mass model with three kinds of time-varying parameters is investigated. Numerical results show that the proposed algorithm has a good capability for tracking the smooth, abrupt, and periodic changes of physical parameters of the system when the response data is corrupted with noise. There is no false alarm in the identified results for all other time-invariant physical parameters. The identification errors become smaller when the signal-noise-ratio increases. The estimated results from free responses are, in general, more accurate than those estimated from random responses at the same noise level. The estimated stiffness coefficients have a better accuracy than that with the estimated damping coefficients.

Acknowledgments

This research is supported by the National Natural Science Foundation of China through Grant No. 10372041, the Natural Science Foundation of Jiang Su Province through Grant No. BK2006520, and a research grant from Hong Kong Polytechnic University Grant No. G-YX26.

References

- [1] Doubling, S. W., Farrar, C. R., and Prime, M. B., "Summary Review of Vibration-Based Damage Identification Methods," *Shock Vibration Diagnosis*, Vol. 30, No. 2, 1998, pp. 91–105.
- [2] Alvin, K. F., Robertson, A. N., Reich, G. W., and Park, K. C., "Structural System Identification: from Reality to Models," *Computers and Structures*, Vol. 81, No. 2003, 2003, pp. 1149–1176.
- [3] Shi, Z. Y., Law, S. S., and Zhang, L. M., "Optimum Sensor Placement for Structural Damage Detection," *Journal of the Engineering Mechanics Division, ASCE*, Vol. 126, No. 11, 2000, pp. 1173–1179.
- [4] Shi, Z. Y., Law, S. S., and Zhang, L. M., "Structural Damage Detection from Modal Strain Energy Change," *Journal of the Engineering Mechanics Division, ASCE*, Vol. 126, No. 12, 2000, pp. 1216–1223.
- [5] Shi, Z. Y., Law, S. S., and Zhang, L. M., "Improved Damage Quantification from Elemental Modal Strain Energy Change," *Journal of the Engineering Mechanics Division, ASCE*, Vol. 128, No. 5, 2002, pp. 521–529.
- [6] Ibrahim, S. R., and Mikulcik, E. C., "A Time Domain Vibration Test," *Shock and Vibration Bulletin*, Vol. 43, No. 4, 1973, pp. 21–37.
- [7] Ibrahim, S. R., "Modal Confidence Factor in Vibrating Testing," *Journal of Spacecraft and Rockets*, Vol. 15, No. 5, 1978, pp. 313–316.
- [8] Deblauwe, F., Brown, D. L., and Allemang, R. J., "The Polyreference Time Domain Technique," *Proceedings of the Fifth International Modal Analysis Conference*, Society for Experimental Mechanics, London, U.K., 1987, pp. 832–842.
- [9] Juang, J. N., and Pappa, R. S., "An Eigensystem Realization Algorithm for Modal Parameter Identification and Model Reduction," *Journal of Guidance, Control, and Dynamics*, Vol. 8, No. 5, 1985, pp. 583–592.
- [10] Juang, J. N., and Pappa, R. S., "Effect of Noise on Modal Parameters Identified by the Eigensystem Realization Algorithm," *Journal of Guidance, Control, and Dynamics*, Vol. 9, No. 3, 1985, pp. 294–303.
- [11] Longman, R. W., and Juang, J. N., "Recursive Form of the Eigensystem Realization Algorithm for System Identification," *Journal of Guidance, Control, and Dynamics*, Vol. 12, No. 5, 1989, pp. 647–652.
- [12] Liu, K., and Miller, D. W., "Time Domain State-Space Identification of Structural Systems," *Journal of Dynamic Systems, Measurement and Control*, Vol. 117, No. 4, 1995, pp. 608–618.
- [13] King, A. M., Desai, U. B., and Skelton, R. E., "A Generalized Approach to Q -Markov Covariance Equivalent Realizations for Discrete Systems," *Automatica*, Vol. 24, No. 4, 1988, pp. 507–515.
- [14] Liu, K., "Modal Parameter Estimation Using the State-Space Method," *Journal of Sound and Vibration*, Vol. 197, No. 4, 1996, pp. 387–402.
- [15] Overschee, P. V., and Moor, B. D., "N4SID: Subspace Algorithm for the Identification of Combined Deterministic Stochastic System," *Automatica* (Special Issue on Statistical Signal Processing and Control), Vol. 30, No. 1, 1994, pp. 75–93.
- [16] Viberg, M., "Subspace-Based Methods for the Identification of Linear Time-Invariant Systems," *Automatica*, Vol. 31, No. 12, 1995, pp. 1835–1851.
- [17] Overschee, P. V., and Moor, B. D., "A Unifying Theorem for Three Subspace System Identification Algorithms," *Automatica*, Vol. 31, No. 12, 1995, pp. 1853–1864.
- [18] Tasker, F., Bosse, A., and Fisher, S., "Real-Time Modal Parameter Estimation Using Subspace Methods: Applications," *Mechanical Systems and Signal Processing*, Vol. 12, No. 6, 1998, pp. 809–823.
- [19] Chui, N. L. C., and Maciejowski, J. M., "Realization of Stable Models with Subspace Methods," *Automatica*, Vol. 32, No. 11, 1996, pp. 1587–1595.
- [20] Ko, W. J., and Hung, C. F., "Extraction of Structural System Matrices from an Identified State-Space System Using the Combined Measurements of Data," *Journal of Sound and Vibration*, Vol. 249, No. 5, 2002, pp. 955–970.
- [21] Huang, C. F., Ko, W. J., and Tai, C. H., "Identification of Dynamic Systems from Data Composed by Combination of Their Response Components," *Engineering Structures*, Vol. 24, No. 11, 2002, pp. 1441–1450.
- [22] Huang, C. F., Ko, W. J., and Peng, Y. T., "Identification of Modal Parameters from Measured Input and Output Data Using a Vector Backward Auto-Regressive with Exogeneous Model," *Journal of Sound and Vibration*, Vol. 276, Sept. 2004, pp. 1043–1063.
- [23] Feldman, M., "Non-Linear System Vibration Analysis Using Hilbert Transform, 1: Free Vibration Analysis Method FREEVIB," *Mechanical Systems and Signal Processing*, Vol. 8, No. 2, 1994, pp. 119–127.
- [24] Feldman, M., "Non-Linear System Vibration Analysis Using Hilbert Transform, 2: Forced Vibration Analysis Method FORCEVIB," *Mechanical Systems and Signal Processing*, Vol. 8, No. 3, 1994, pp. 309–318.
- [25] Shi, Z. Y., and Law, S. S., "Identification of Linear Time-Varying Dynamical Systems Using Hilbert Transform and EMD Method," *Journal of Applied Mechanics*, Vol. 74, No. 2, 2007, pp. 223–230.
- [26] Loh, C. H., Liu, C. Y., and Huang, C. C., "Time Domain Identification of Frames Under Earthquake Loadings," *Journal of Engineering Mechanics*, Vol. 126, No. 7, 2000, pp. 693–703.
- [27] Kosmatopolous, E. B., Smyth, A. W., Masri, S. F., and Chassiakos, A. G., "Robust Adaptive Neural Estimation of Restoring Forces in Nonlinear Structures," *Journal of Applied Mechanics*, Vol. 68, No. 6, 2001, pp. 880–893.
- [28] Smyth, A. W., Masri, S. F., Kosmatopolous, E. B., Chassiakos, A. G., and Caughey, T. K., "Development of Adaptive Modeling Techniques for Non-Linear Hysteretic Systems," *International Journal of Non-Linear Mechanics*, Vol. 37, No. 8, 2002, pp. 1435–1451.
- [29] Yang, J. N., and Lin, S., "Identification of Parametric Variations of Structures Based on Least Square Estimation and Adaptive Tracking Technique," *Journal of the Engineering Mechanics Division, ASCE*, Vol. 131, No. 3, 2005, pp. 290–298.
- [30] Ghanem, R., and Romeo, F., "A Wavelet-Based Approach for the Identification of Linear Time-Varying Dynamical Systems," *Journal of Sound and Vibration*, Vol. 234, No. 4, 2000, pp. 555–576.
- [31] Zhao, H. P., and Bentsman, J., "Biorthogonal Wavelet Based Identification of Fast Linear Time-Varying Systems, Part 1: System Representations," *Journal of Dynamic Systems, Measurement, and Control*, Vol. 123, No. 4, 2001, pp. 585–592.
- [32] Liu, K., "Identification of Linear Time-Varying Systems," *Journal of Sound and Vibration*, Vol. 206, No. 4, 1997, pp. 487–505.
- [33] Liu, K., "Extension of Modal Analysis to Linear Time-Varying Systems," *Journal of Sound and Vibration*, Vol. 226, No. 1, 1999, pp. 149–167.
- [34] Liu, K., and Deng, L., "Experimental Verification of an Algorithm for Identification of Linear Time-Varying Systems," *Journal of Sound and Vibration*, Vol. 279, Jan. 2005, pp. 1170–1180.
- [35] Shokoohi, S., and Silverman, L., "Identification and Model Reduction of Time-Varying Discrete-Time Systems," *Automatica*, Vol. 23, No. 4, 1987, pp. 509–521.
- [36] Verhaegen, M., and Yu, X., "A Class of Subspace Model Identification Algorithms to Identify Periodically and Arbitrarily Time-Varying Systems," *Automatica*, Vol. 31, No. 2, 1995, pp. 201–216.
- [37] Basseville, M., Benveniste, A., Moustakides, G., and Rougee, A., "Detection and Diagnosis of Changes in the Eigenstructure of Nonstationary Multivariable Systems," *Automatica*, Vol. 23, No. 4, 1987, pp. 479–489.